

Electronic Supplementary Information

Pyrene-functionalized tungsten disulfide as stable resistive photosensor

Ruben Canton-Vitoria,^{a} Sebastian Nufer^{b, c} Xiaoyang Che^{d, e,}
Yuman Sayed-Ahmad Baraza,^d Raul Arenal,^{f, g, h*} Carla
Bittencourt,^{i*} Adam Brunton,^b Alan B. Dalton,^c Christopher P.
Ewels,^{d*} Nikos Tagmatarchis^{a*}*

¹ Theoretical and Physical Chemistry Institute, National Hellenic Research Foundation, 48 Vassileos Constantinou Avenue, 116 35 Athens, Greece.

² M-Solv Ltd, Oxonian Park, Langford Locks, Kidlington, Oxford, OX5 1FP, United Kingdom.

³ Department of Physics, University of Sussex, Brighton, BN1 9R, United Kingdom.

⁴ Institut des Materiaux Jean Rouxel (IMN), UMR6502 CNRS, Universite de Nantes, 2 Rue de la Houssiniere, BP32229, 44322 Nantes, France.

⁵ Centre de Recherche Paul Pascal (CRPP)-UMR5031, 115 Avenue du Dr. Albert Schweitzer, 33600 Pessac, France.

⁶ Laboratorio de Microscopias Avanzadas (LMA), Universidad de Zaragoza, Calle Mariano Esquillor, 50018 Zaragoza, Spain.

⁷ Fundacion ARAID, 50018 Zaragoza, Spain.

⁸ Instituto de Nanociencia y Materiales de Aragón (INMA), CSIC-Universidad de Zaragoza, Calle Pedro Cerbuna, 50009 Zaragoza, Spain.

⁹ Chimie des Interactions Plasma-Surface, University of Mons, 20 Place du Parc, 7000 Mons, Belgium.

***Correspondence**

tagmatar@eie.gr (N. Tagmatarchis)

1 Sample Characterisation Techniques

UV-Vis absorption spectra were recorded on a PerkinElmer (Lambda 19) UV-Vis-NIR spectrophotometer. Steady-state UV-Vis electronic absorption spectra were recorded on a PerkinElmer (Lambda 19) UV-Vis-NIR spectrophotometer.

Steady-state emission spectra were recorded on a Fluorolog-3 JobinYvon-Spex spectrofluorometer (model GL3-21).

Pico-second time-resolved fluorescence spectra were measured by the time-correlated-single-photon-counting (TCSPC) method on a Nano-Log spectrofluorometer (Horiba JobinYvon), using a laser diode as an excitation source (NanoLED, 375 nm) and a UV-Vis detector TBX-PMT series (250-850 nm) by Horiba JobinYvon. Lifetimes were evaluated with the DAS6 Fluorescence-Decay Analysis Software.

Mid-infrared spectra in the region 500–4500 cm^{-1} were obtained on a Fourier transform IR spectrometer (Equinox 55 from Bruker Optics) equipped with a single reflection diamond ATR accessory (DuraSamp1IR II by SensIR Technologies). A drop of the solution was placed on the diamond surface, followed by evaporation of the solvent, in a stream of nitrogen, before recording the spectrum. Typically, 100 scans were acquired at 2 cm^{-1} resolution.

Micro-Raman scattering measurements were performed at room temperature in the backscattering geometry using a RENISHAW in Via Raman microscope equipped with a CCD camera and a Leica microscope. A 2400 lines mm^{-1} grating was used for all measurements, providing a spectral resolution of $\pm 1 \text{ cm}^{-1}$. As an excitation source an Ar^+ laser (514 nm with less than 4.5 mW laser power) was used. Measurements were taken with 10 seconds of exposure times at varying numbers of accumulations. The laser spot was focused on the sample surface using a long working distance 50 \times objective. Raman spectra were collected on numerous spots on the sample and recorded with Peltier cooled CCD camera. The data were collected and analyzed with Renishaw Wire and Origin software.

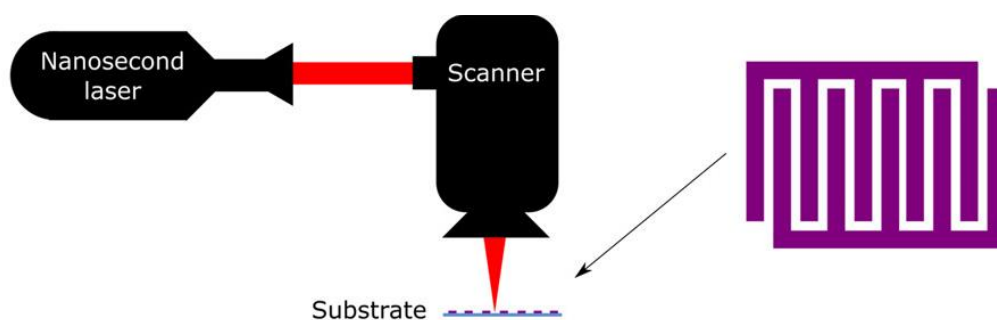
Thermogravimetric analysis was performed using a TGA Q500 V20.2 Build 27 instrument by TA in a nitrogen (purity >99.999%) inert atmosphere.

X-ray photoelectron analysis (XPS) was performed with a Kratos AXIS Supra. The spectra were obtained using a monochromatized Al-K α source at 1486.6 eV running at 15 kV and 10 mA. The survey spectrum was measured at 160 eV pass energy and for the individual peak regions, spectra were recorded with pass energy of 20 eV. The energy resolution was < 0.48 eV. The analysis of peaks was performed with the Casa XPS software, using a weighted sum of Lorentzian and Gaussian components curves after Shirley background subtraction. The binding energies were referenced to the internal C1s standard at 284.6 eV.

High-resolution scanning transmission electron microscopy (HRSTEM) and electron energy-loss spectroscopy (EELS) have been conducted using an aberration-corrected FEI Titan Low-Base microscope operated at 80 kV. This microscope is equipped with a C_s probe corrector and a Gatan Tridiem ESR 865 EELS spectrometer. The energy resolution was $\sim 1 \text{ eV}$. The convergence and collection angles were 25 and 80 mrad, respectively.

2 Photoresistor Design and Operation

The substrates used in the devices were obtained from AimCore Technology (Hsinchu 30351, Taiwan); these consist of a glass substrate sputtered with molybdenum forming a 700 nm thick metallic layer. An infrared nanosecond laser (Multiwave, set to 10 ns, 1064 nm) and a galvoscaner were used to pattern the interdigitated electrodes (IDEs) into the metal, following the procedure detailed in [ACS Appl. Mater. Interfaces, 10, 21740, 2018]. The laser was used in focus with a fluence of 3 J cm^{-2} at a mark speed of 1000 mm s^{-1} . The finger electrode pattern was designed in a drawing interchange format (DXF) format created in a computer-aided design to feed to the scanner. A Keithley 2420 SourceMeter and LabVIEW were used to measure the device resistance over time.



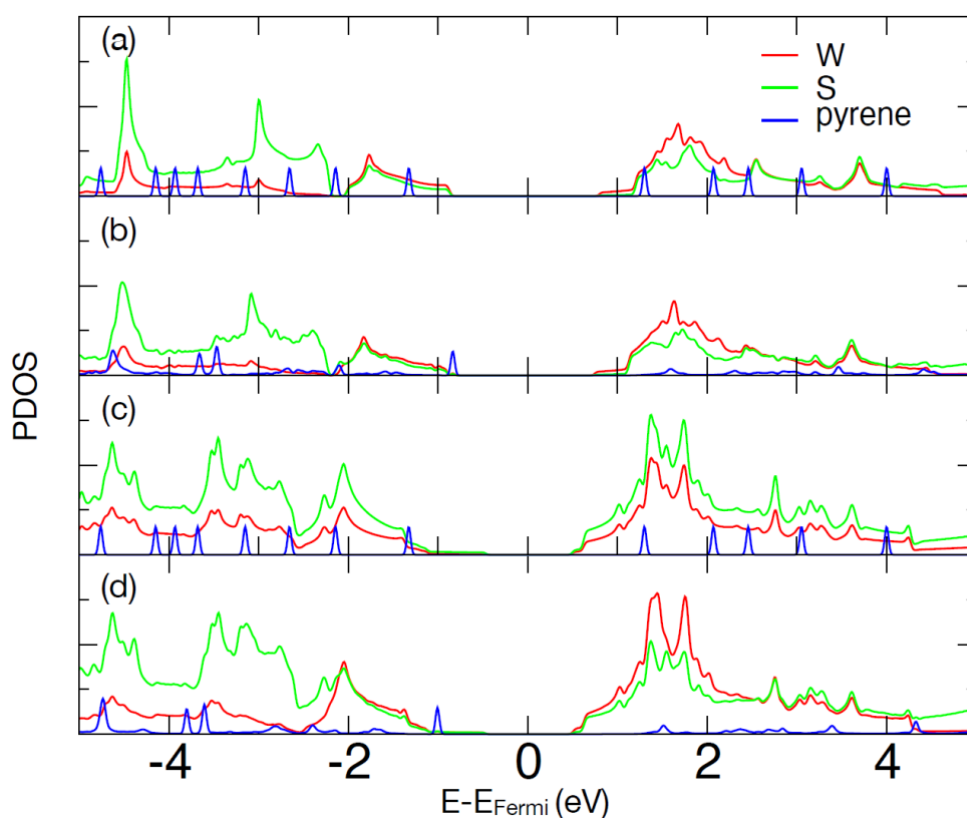
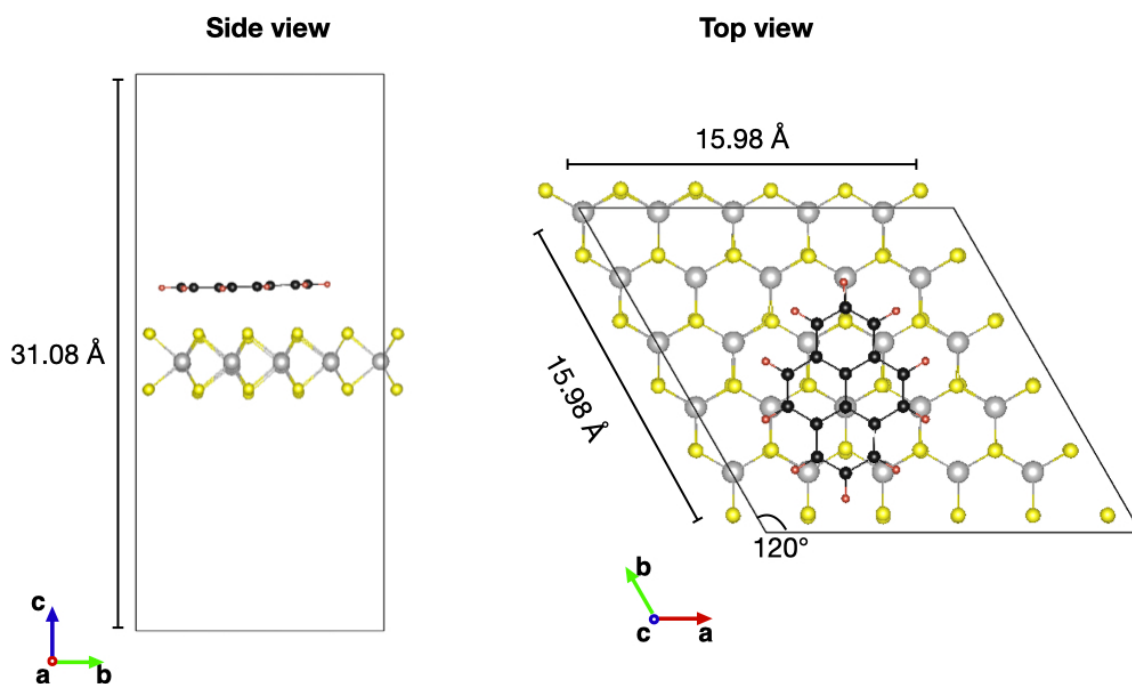


Figure S1. (top) Unit cell used for calculation of pyrene on the surface of WS₂. Multiple initial pyrene orientations and locations were tested, the figure shows the most stable configuration obtained. (bottom) Calculated projected density of electronic states for (a) monolayer WS₂ and pyrene at infinite separation, (b) pyrene on monolayer WS₂ surface in ground state, (c, d) bilayer WS₂ with pyrene at (c) separate and (d) surface bound. Energies are shifted to place the Fermi level at 0 eV in each case, states localized on W/S/pyrene are marked in red/green/blue, respectively

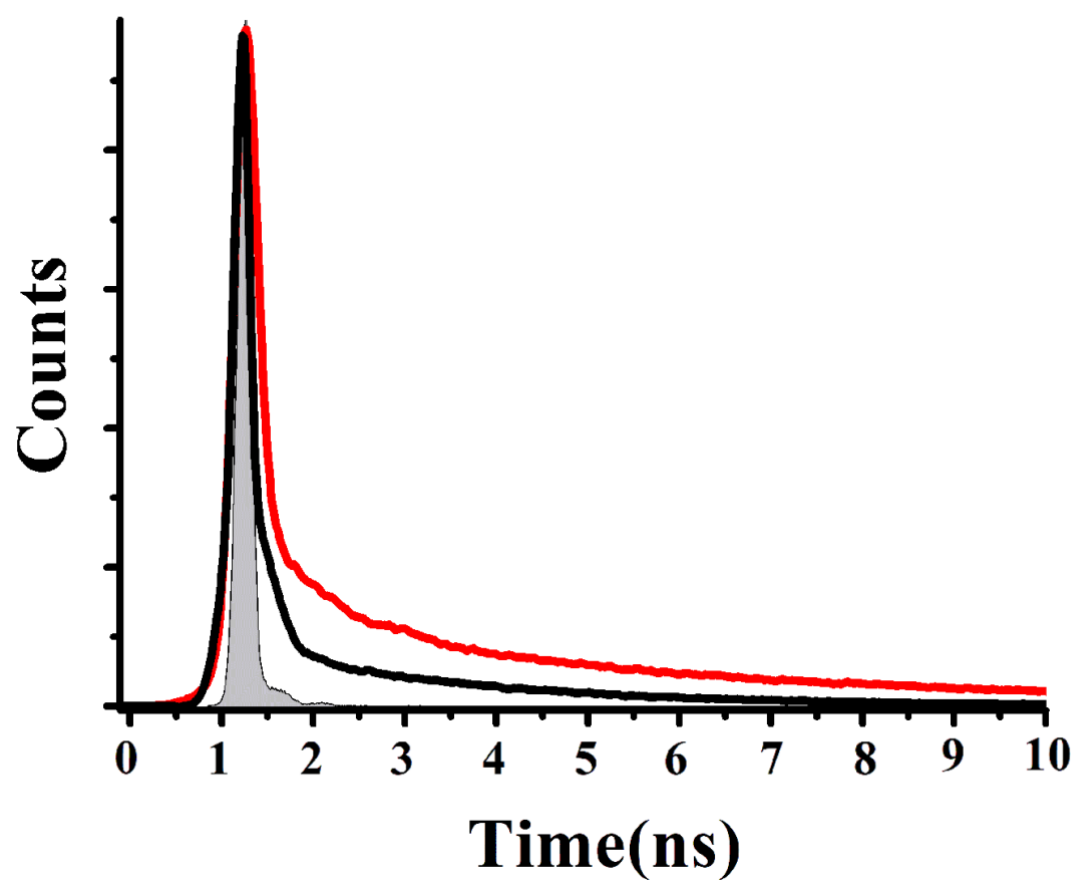


Figure S2. Decay lifetime (λ_{exc} 376 nm; λ_{em} 396 nm) for pyrene derivative **1** (red) and hybrid material **2** (black), obtained in DMF.

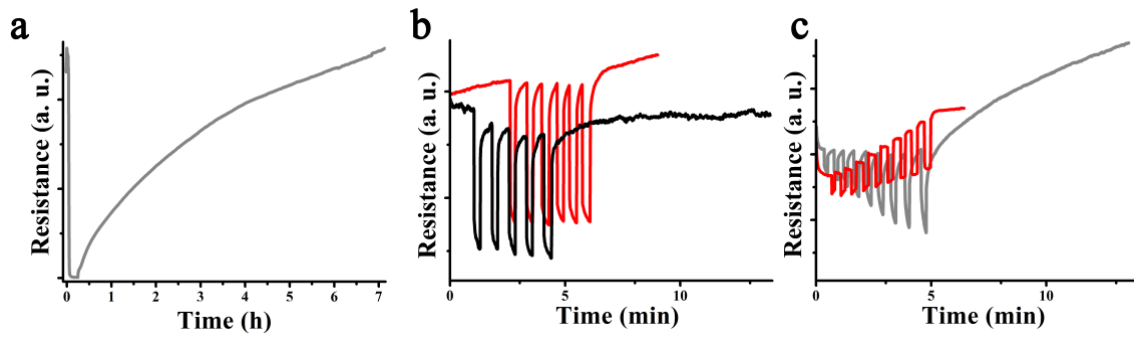


Figure S3. a) Resistance change for exfoliated WS₂ during several hours of moisture induction due to atmosphere conditions changes. b) Resistance change for WS₂-pyrene hybrid material **2** under air (red) and with Scotch tape protection (black) and c) exfoliated WS₂ under air (red) and with Scotch tape protection (gray) during light pulses at 600 mW/cm².

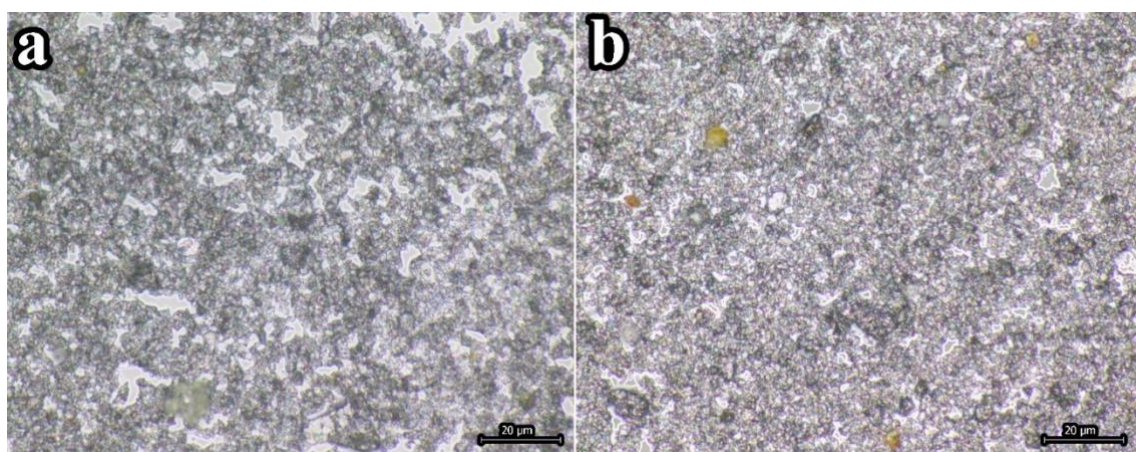


Figure S4. Optical micrographs of (a) exfoliated WS₂ and (b) material **2** showing homogenous material distribution over the sensor surface.

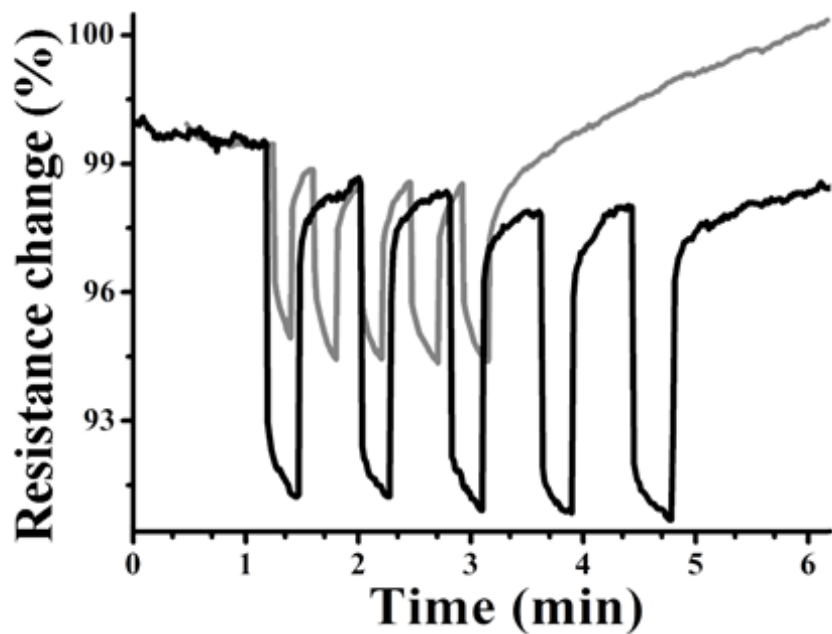


Figure S5. Resistance response of hybrid material 2 (black) and exfoliated WS₂ (gray) protected by Scotch tape and upon repeated light irradiation with an intensity of 600 mW/cm².

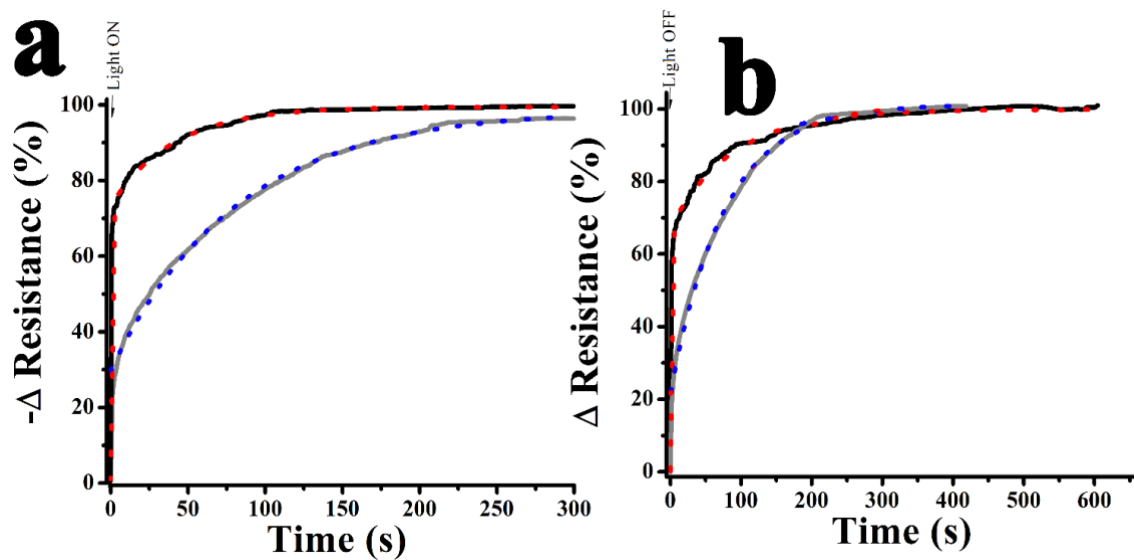


Figure S6. Variation of (a) resistance response and (b) recovery resistance response for hybrid material **2** (black) and exfoliated WS₂ (gray) protected by Scotch tape and the corresponding monoexponential (red) and biexponential (blue) fitting with repeated light at 600 mW/cm². Graphs were subtracted from Fig. 7b after extracting drift.

Response lifetimes					
	T ₁ (s)	T ₂ (s)	A ₁ (%)	A ₂ (%)	R ₂
Exfoliated WS ₂	77.8		100		0.991
Material 2	26.3		100		0.775
	39.0	0.37	26	73	0.995
Response recovery lifetimes					
	T ₁ (s)	T ₂ (s)	A ₁ (%)	A ₂ (%)	R ₂
Exfoliated WS ₂	76.1		100		0.992
Material 2	55.9		100		0.840
	80.7	0.90	32	68	0.991

Table 1. Fitting parameters of response and response decay in Fig. S7 using monoexponential and biexponential fits (R₂-values shows quality of the fits given and necessity for a biexponential fit for Material 2). Response lifetimes fitted to:

Monoexponential:

$$(S1): |A_t| = A_0 - A_0 e^{-\frac{1}{T_2}t} + C \quad \text{and: } A_0 = A_1$$

Biexponential:

$$(S1): |A_t| = A_0 - (A_0 - A_2)e^{-\frac{1}{T_1}t} - A_2 e^{-\frac{1}{T_2}t} + C \quad \text{and: } A_0 = A_1 + A_2$$

Wherein: T₁ and T₂ are the resistance lifetimes; t is the time; A_t is the variation of the resistance respect the time; A₀ is the maximum variation of resistance; A₁ and A₂ the maximum variation of the resistance related with the population of lifetime; and C is a constant necessary for calculate the position but without physical meaning. Noted that A₀=A₁+A₂, and A₁ has been substituted in order to reduce the number of parameters.